Catalytic intramolecular hydroamination of aminoallenes using titanium complexes of chiral, tridentate, dianionic imine-diol ligands

Fanrui Sha[‡], Benjamin S. Mitchell[†], Chris Z. Ye[‡], Chase S. Abelson[†], Eric W. Reinheimer[§], Pierre LeMagueres[§], Joseph D. Ferrara[§], Michael K. Takase[‖], and Adam R. Johnson[‡,*]

[†]WM Keck Science Department, Claremont McKenna, Pitzer, and Scripps Colleges, Claremont, CA 91711

[‡]Harvey Mudd College, 301 Platt Blvd., Claremont, CA 91711

[§]Rigaku Americas Corporation, 9009 New Trails Drive, The Woodlands, TX 77381

[‖]Beckman Institute, California Institute of Technology, Pasadena, CA 91125

Abstract

Alkylation of D- or L-phenylalanine or valine alkyl esters was carried out using methyl or phenyl Grignard reagents. Subsequent condensation with salicylaldehyde, 3,5-di-*tert*-butylsalicylaldehyde, or 5-fluorosalicylaldehyde formed tridentate, X_2L type, Schiff base ligands. Chiral shift NMR confirmed retention of stereochemistry during synthesis. X-ray crystal structures of four of the ligands show either inter- or intramolecular hydrogen bonding interactions. The ligands coordinate to the titanium reagents $Ti(NMe_2)_4$ or $TiCl(NMe_2)_3$ by protonolysis and displacement of two equivalents of $HNMe_2$. The crystal structure of one example of $Ti(X_2L)Cl(NMe_2)$ was determined and the complex has a distorted square pyramidal geometry with an axial NMe_2 ligand. The *bis*-dimethylamide complexes are active catalysts for the ring closing hydroamination of di- and trisubstituted aminoallenes. The reaction of hepta-4,5-dienylamine at 135 °C with 5 mol% catalyst gives a mixture of 6-ethyl-2,3,4,5-

tetrahydropyridine (40-72%) and both *Z*- and *E*-2-propenyl-pyrrolidine (25-52%). The ring closing reaction of 6-methyl-hepta-4,5-dienylamine at 135 °C with 5 mol% catalyst gives exclusively 2-(2-methyl-propenyl)-pyrrolidine. The pyrrolidine products are obtained with enantiomeric excesses up to 17%.

Introduction

Piperidine and pyrrolidine are the first- and fifth-most common nitrogen ring structures in US FDA approved pharmaceuticals, and of these, most are substituted at the N_1- and C_2-positions.[1] Hydroamination, the formal addition of an N-H bond across a C=C unsaturated bond, is an attractive method for the synthesis of these heterocycles and other nitrogen containing products as the reaction is 100% atom economical.[2-12] The intermolecular hydroamination of alkenes and alkynes with aliphatic and aromatic amines has been developed with a special emphasis in obtaining the anti-Markovnikov product, as this transformation is more difficult to achieve and linear amines are of more value.[13-15] The intramolecular hydroamination-cyclization of aminoallenes, -alkenes, and -alkynes has been examined for the formation of nitrogen-containing heterocycles. While the addition to aminoalkynes is more thermodynamically facile,[16, 17] the addition to aminoallenes and -alkenes can give rise to cyclic products with a chiral center, making the development of this latter reaction more attractive.

There has been a resurgence of interest in the use of the earth abundant, non-toxic, and relatively inexpensive group-IV metals for catalytic reactions.[18] Titanium is an abundant and sustainable transition metal,[19] and its principal byproduct, TiO_2, is non-toxic. For hydroamination (and the closely related hydroaminoalkylation),[20] the groups of Doye,[21] Hultzsch,[22] Odom,[23-26] Roesky,[27, 28] Sadow,[29, 30] Schafer,[31-34] and Xie,[35, 36] among others,[37] have reported on both the inter- and intramolecular reaction using titanium and zirconium catalysts.

Tonks has been influential in recent years highlighting the use of titanium with redox non-innocent ligands for cycloaddition reactions and nitrene transfer.[38-40]

Our laboratory is interested in the development of catalysts for asymmetric hydroamination using earth-abundant metals with non-toxic byproducts. Our group reported this reaction with both di- and trisubstituted aminoallenes (Scheme 1, compounds **1a** and **1b**) in 2004,[41] using bidentate amide-alkoxide complexes of titanium. For substrate **1a**, tetrahydropyridine **2a** was obtained in approximately 1:2-4 ratio with pyrrolidine **3a**. Substrate **1b** gives exclusively the pyrrolidine **3b**, and catalysts derived from sterically encumbered amino alcohols gave higher enantioselectivities, up to 16% ee.[42] These same ligands on tantalum gave significantly higher enantioselectivity, up to 80% ee.[43, 44]

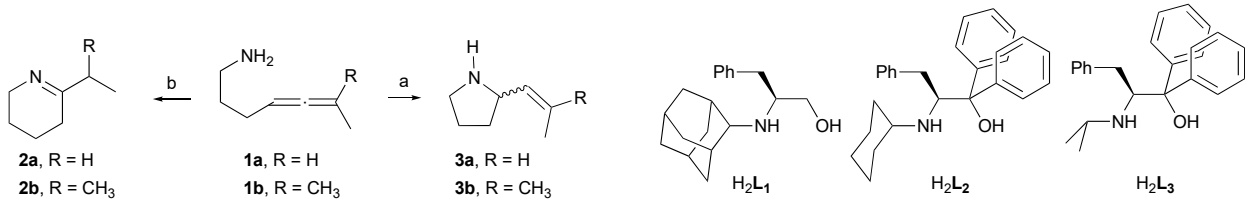

3a: 16 %ee with Ti(**L**$_1$)(NMe$_2$)$_2$
3b: 15 %ee with Ti(**L**$_1$)NMe$_2$)$_2$, 16 %ee with Ti(**L**$_2$)(NMe$_2$)$_2$, Ti(**L**$_3$)(NMe$_2$)$_2$
3b: 80 %ee with Ta(**L**$_3$)(NMe$_2$)$_2$

Scheme 1. Catalytic asymmetric hydroamination of di- and trisubstituted aminoallenes (1) to give achiral tetrahydropyridines (2) or chiral α-vinylpyrrolidines (3). The highest enantioselectivities were obtained with the three ligands shown: H$_2$L$_1$, H$_2$L$_2$, and H$_2$L$_3$.

In 2007, Toste reported the enantioselective gold phosphine catalyzed hydroamination-cyclization of trisubstituted aminoallenes, including the *N*-tosylated derivative of substrate **1b**, to give pyrrolidines with enantioselectivities up to 99% ee.[45] There are three important differences with our catalytic system. First, we use the early and earth abundant metal titanium in our catalysts. Second, our substrates are unprotected amines leading to unprotected secondary pyrrolidine products; most examples of aminoallene hydroamination by metals other than lanthanides[8] or group-IV metals require the use of *N*-protected substrates,[10, 46, 47] which must be

deprotected in an additional step to obtain the secondary amine product. Third, the synthesis of complex chiral ligands such as Toste's (*R*)-3,5-xylyl-BINAP, requires multiple steps and chiral resolving agents.[48, 49] All three of these factors make the current state-of-the-art methods for aminoallene hydroamination less green than they could be.[50] Further development of titanium catalysts, especially those with ligands derived from the chiral pool,[51] is required in order to decrease the environmental impact and improve the enantioselectivity of the reaction.

The titanium complexes of bidentate amino alcohols we have prepared previously are all dimeric TiX_4L complexes with bridging alkoxide oxygen atoms in both the solid state and in solution based on crystallographic and spectroscopic characterization (Chart 1a).[41, 52, 53] On the other hand, the tantalum complexes of these same ligands are monomeric TaX_5 complexes (Chart 1b).[43] As the tantalum complexes give much higher enantioselectivities for the hydroamination reaction, we postulated that incorporating a neutral donor ligand, thus forming a tridentate ligand of similar design, would break the dimers apart into monomeric TiX_4L complexes, allowing the titanium complexes to behave more like their monomeric group-V counterparts (Chart 1c).

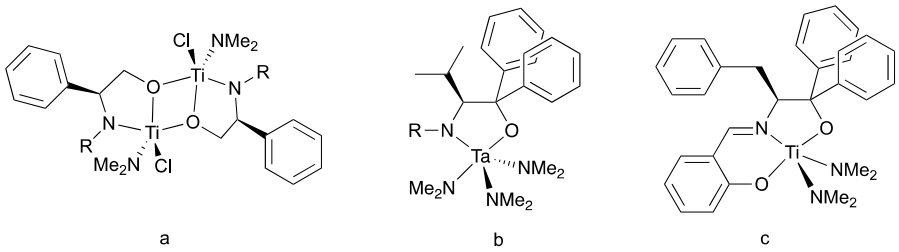

Chart 1. Structures of (a) dimeric titanium complexes (b) monomeric tantalum complexes with bidentate amide alkoxide ligands, and (c) monomeric titanium complexes with tridentate imine dialkoxide ligands; structures derived from X-ray crystallographic and spectroscopic data.

Based on this design principle, we devised the modular synthesis of a readily prepared tridentate ligand. We combined chiral aminoalcohols with substituted salicylaldehydes in order

to prepare a tridentate XLX[54] ligand. The ligand is derived from chiral pool building blocks and commercially available aldehyde coupling partners. Salicylaldehydes were deemed appropriate coupling partners as the similarly derived salen ligands are used across the transition metal series to stabilize metals and provide an asymmetric environment for catalysis.[55, 56] With an imine nitrogen and phenoxide and alkoxide oxygen donor atoms, this tridentate ligand is well-suited to bind to an oxophilic titanium center while providing steric and electronic sites on the aromatic ring and ligand backbone to change the coordination environment around the metal center. Several examples of this ligand class have been prepared previously,[57] and they have been used successfully as supporting ligands for copper[58, 59] and titanium[60, 61] catalyzed alkylation reactions. Xie reported very similar ligands derived from the condensation of proline or O-alkylated valine with substituted salicylaldehydes.[35] They observed high enantioselectivities (above 90%) with this ligand for the zirconium catalyzed asymmetric hydroamination of a number of *gem*-dialkylsubstituted aminoalkenes. We prepared a number of sterically and electronically differentiated tridentate ligands and their titanium complexes in an attempt to achieve high enantioselectivity in the hydroamination of aminoallene substrates with titanium catalysts.

Results and Discussion

Design and synthesis of ligands

Synthetically, the incorporation of an L-type ligand between two X-type ligands was straightforward. The methyl or ethyl esters of L-phenylalanine or L-valine can be alkylated with either methyl or phenyl Grignard at 0 °C in ether affording the known aminoalcohols (*S*)-2-amino-1,1,3-triphenylpropanol,[62, 63] (*S*)-2-amino-3-phenyl-l,1-dimethylpropanol[64] or (*S*)-2-amino-3-methyl-1,1-diphenylbutanol in 63-87% yields (Scheme 2).[62] The amines can then be

condensed with the commercially available salicylaldehyde, 3,5-di-*tert*-butylsalicylaldehyde or 5-fluorosalicylaldehyde in ethanol at reflux to give the ligands L-H_2**L4**, L-H_2**L5**, L-H_2**L6**, L-H_2**L7**, and L-H_2**L8** that could be purified by recrystallization or chromatography. For H_2**L6**, purification was more difficult, unless a deficiency of aldehyde (0.9 equiv) was used during the synthesis. The D-enantiomers were prepared in a similar fashion from the appropriate D-amino acid ester precursors. These aldehydes were chosen to allow us to readily explore the steric, and to a lesser extent, electronic effects of ligand substitution on hydroamination activity and selectivity. In our prior studies, sterically more encumbered ligands gave higher enantioselectivity.[43]

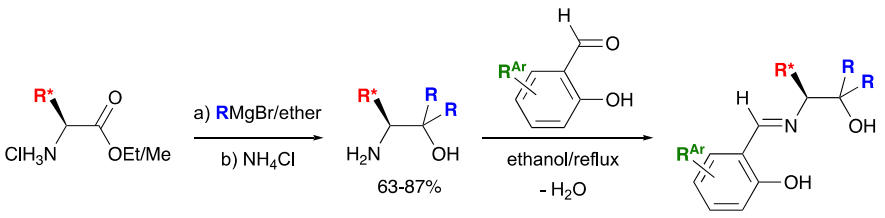

ligand	H_2**L4**	H_2**L5**	H_2**L6**	H_2**L7**	H_2**L8**
R	Me	Ph	Ph	Ph	Ph
R*	CH_2Ph	CH_2Ph	CH_2Ph	CH_2Ph	$CHMe_2$
R^{Ar}	H	H	3,5-di-*tert*-butyl	5-F	5-F
yield	56%	62%	42%	60%	35%

Scheme 2. Synthesis of tridentate XLX ligands; reported yield is after purification

Both L-H_2**L5** and L-H_2**L6** have been reported in the literature previously.[57] However, neither compound was characterized by optical rotation, melting point or mass spectrometry. In addition, the ^{1}H NMR spectrum for L-H_2**L6** did not have an assignment for the imine proton resonance, and one of the coupling constants is incorrect. The experimental section provides complete characterization, including Mp, $[\alpha]_D$ and MS, of the newly and the previously reported ligands, and correct coupling constants for L-H_2**L6**. The optical rotations for all five L-ligands are approximately equal and opposite to that of the D-enantiomers, as expected.

Previously in our laboratory, we have observed partial racemization during alkylation using a Grignard reagent with phenylglycine based ligands ($R^* = Ph$).[41] The presence of a benzylic hydrogen at the chiral center renders these ligand precursors susceptible to deprotonation/epimerization during synthesis. As a precaution against racemization, the alkylation reactions were carried out at low temperature (0 °C). In addition, chiral contact shift NMR experiments were carried out to demonstrate the presence of only a single enantiomer. Treatment of a ligand with one equivalent of (*S*)-(+)-2,2,2-Trifluoro-1-(9-anthryl)ethanol in $CDCl_3$ resulted in chemical shift changes of ca. 0.02-0.1 ppm due to the diastereomeric hydrogen bonded complex (see experimental section for details).[65] No splitting of the peaks was observed until the corresponding solution of the D-enantiomer of the ligand was added, in which case both diastereomers were observed by NMR spectroscopy. The lack of splitting of the peaks is strong evidence that there was no racemization during the synthesis. Plots of well-resolved regions of the NMR spectrum demonstrating this behavior are included in the ESI.

Solid-state structures of ligands

Four of the five ligands were characterized by X-ray crystallography. L-H_2**L4**, L-H_2**L6**, L-H_2**L7**, and L-H_2**L8** each crystallized from 4:1 ether:isopropanol to give X-ray quality crystals. The molecular structure of L-H_2**L4** is shown in Figure 1, and pertinent crystallographic parameters are listed in Table 1. Rather than the expected imino-phenol tautomer, the crystal structure clearly showed the iminium-phenoxide tautomer, with the iminium N atom protonated and the phenol O atom deprotonated. There is an intramolecular hydrogen bond between N(1) and the phenoxide oxygen, O(1). Previously we have observed intramolecular hydrogen bonds between the aliphatic oxygen and the amine nitrogen in our bidentate amino alcohols.[66, 67]

Table 1. Crystal Data and Structure Refinement for L-H_2L4, L-H_2L6, L-H_2L7, L-H_2L8 and 14

Compound	L-H_2L4	L-H_2L6	L-H_2L7	L-H_2L8	14
CCDC code	1837506	1837507	1837508	1837509	1834567
Formula	$C_{18}H_{21}NO_2$	$C_{36}H_{41}NO_2$	$C_{28}H_{24}FNO_2$	$C_{24}H_{24}FNO_2$	$C_{41}H_{51}Cl_7N_2O_2Ti$
Formula weight	283.36	519.7	425.48	377.44	899.89
Temperature, K	100(2)	100(2)	100(2)	100(2)	100(2)
Wavelength, Å	Cu Kα, 1.54184	Cu Kα, 1.54184	Cu Kα, 1.54184	Cu Kα, 1.54184	Mo Kα, 0.71073
Space group	$P2_12_12_1$	$P2_12_12_1$	$P2_12_12_1$	$P2_12_12_1$	$P2_12_12_1$
a, Å	6.27660(10)	9.77210(10)	5.93196(5)	6.12710(10)	12.3004(7)
b, Å	13.5578(2)	11.08970(10)	18.49475(19)	16.0917(3)	15.5000(7)
c, Å	17.4247(2)	27.2621(2)	20.30007(19)	19.7246(4)	23.3578(12)
α, °	90.00	90.00	90.00	90.00	90.00
β, °	90.00	90.00	90.00	90.00	90.00
γ, °	90.00	90.00	90.00	90.00	90.00
volume, Å^3	1482.79(4)	2954.38(5)	2227.12(4)	1944.76(6)	4453.3(4)
Z	4	4	4	4	4
Density (calculated), mg/m^3	1.269	1.168	1.269	1.289	1.34
μ, mm^{-1}	0.651	0.548	0.685	0.710	0.648
Scan	ω scan	ω scan	ω scan	ω scan	ϕ and ω scan
θ range for data collection, °	6.038-66.550	4.304-67.072	4.356-67.058	5.940-66.600	2.287-36.460
Reflections measured	13819	27404	20287	17736	76119
Independent observed reflns.	2621	5277	3962	3439	21602
Independent reflns. [$I>2\sigma$]	2596	5186	3901	3251	18114
Data/restraints/parameters	2621/0/275	5277/48/386	3962/0/298	3439/0/350	21602/217/541
R_{int}	0.0283	0.0294	0.0337	0.0478	0.0584
Final R Indices [$I>2\sigma$]	R_1 = 0.0229, $wR2$ = 0.0585	R_1 = 0.0272, $wR2$ = 0.0683	R_1 = 0.0240, $wR2$ = 0.0603	R_1 = 0.0265, $wR2$ = 0.0641	R_1 = 0.0553 $wR2$ = 0.1407
R Indices (all data)	R_1 = 0.0231, $wR2$ = 0.0587	R_1 = 0.0277, $wR2$ = 0.0686	R_1 = 0.0244, $wR2$ = 0.0605	R_1 = 0.0290, $wR2$ = 0.0651	R_1 = 0.0692 $wR2$ = 0.1509
Goodness-of-fit on F^2	1.053	1.041	1.069	1.055	1.036
Flack Parameter	-0.03(7)	-0.04(5)	0.06(4)	-0.07(9)	0.016(8)
Largest diff peak/hole, e Å^{-3}	0.145/-0.140	0.197/-0.209	0.178/-0.133	0.163/-0.113	1.209/-1.106

The atoms in the phenoxide aromatic ring, O(1), C(7), N(1) and H(1), are all essentially coplanar. There is a significant difference in the bond lengths from C(1)-O(1), at 1.2944(19) Å and C(9)-O(2), at 1.4240(18) Å, suggesting that a more accurate description of the structure is the keto-iminium ion with delocalization of charge along C(1)-C(6)-C(7)-N(1). There is residual electron density in the electron density map around C(6), suggesting a buildup of negative charge at that atom. The bonds between C(1)-C(2), C(1)-C(6), C(3)-C(4) and C(5)-C(6) are all long, at 1.410 – 1.440 Å, while the C(2)-C(3) and C(4)-C(5) bond lengths are both shorter at around 1.37 Å. In contrast, the C-C bond lengths in the aromatic ring on the benzyl side chain are typical aromatic bond distances ranging from 1.383 to 1.394 Å.

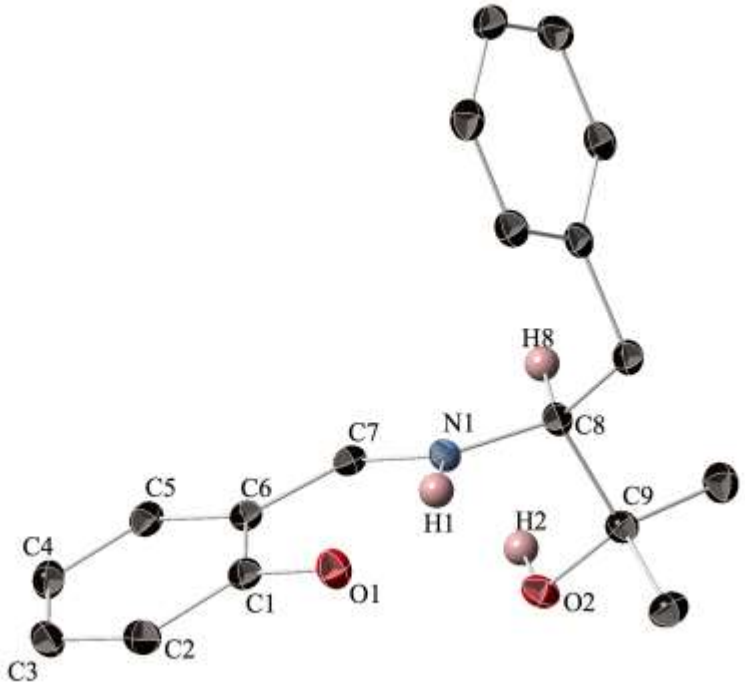

Figure 1. Thermal ellipsoid drawing of L-H_2L4 (hydrogen atoms except H(1), H(2) and H(8) are omitted for clarity; ellipsoids shown at 50% probability). Selected bond distances (Å): C(1)-C(2) 1.418(2), C(2)-C(3) 1.373(2), C(3)-C(4) 1.410(2), C(4)-C(5) 1.368(2), C(5)-C(6) 1.416(2), C(6)-C(1) 1.440(2), C(1)-O(1) 1.2944(19), C(9)-O(2) 1.4240(18), C(7)-N(1) 1.302(2).

The iminium phenoxide structure has been observed previously for imino phenols.[68] An interesting example by Salehi[69] has two similar structures exhibiting both possible tautomeric forms. One structure in that paper has the imino-phenol structure (HL^1), while another exhibits the iminium-phenoxide structure (HL^2). HL^2 has the deprotonated phenol oxygen engaged in both inter- and intramolecular H bonds to iminium hydrogens and has almost exactly the same C-C and C-O bond lengths as seen in L-H_2**L4**. Examining the intermolecular contacts of L-H_2**L4** shows that in addition to the intramolecular hydrogen bonding, there is a similar network of intermolecular hydrogen bonding of H(2) to O(1) of a neighboring molecule. The ESI contains a figure illustrating this network.

As this structure was unexpected, density functional calculations were carried out on both tautomers with Gaussian using the B3LYP functional and the 6-31G(d,p) basis set.[70] As expected, the vacuum phase imine-phenol tautomer was calculated to be lower in energy than the iminium phenoxide tautomer by approximately 4 kcal/mol. The offset in energy stabilization by the intermolecular hydrogen bonding network is apparently enough to favor the higher energy structure. Details of the calculations are provided in the ESI.

The molecular structure of L-H_2**L6** is shown in Figure 2. The molecule crystallized with the expected imine-phenol tautomer structure, and contains an intramolecular hydrogen bond between N(1) and O(2). As with L-H_2**L4**, the atoms in the phenoxide aromatic ring, O(2), H(2), C(22) and N(1), are all essentially coplanar. The diphenyl substitution on the aliphatic alcohol group prevents intermolecular contacts involving O(1). Some of our bidentate amino alcohol ligands have exhibited intermolecular hydrogen bonding when the aliphatic oxygen is primary,[66] but not when it is tertiary.[66, 67] Aside from the intramolecular hydrogen bond between O(2)-H(2)-N(1), there are no additional contacts with the atoms H(2), O(1), O(2) or N(1) within 3Å. As seen in the structure of L-H_2**L4**, there is a significant difference in the bond lengths from C(24)-O(2), at 1.3570(18) Å, and C(1)-O(1), at 1.4323(19) Å. The bonds between C(24)-C(23), C(23)-C(28), C(27)-C(26) and C(24)-C(25) are all long, at 1.400 – 1.412 Å, while the C(28)-C(27) and C(26)-C(25) bonds are both shorter at around 1.39 Å. The differences in bond-lengths between the phenol aromatic ring and the side chain aromatic ring are less pronounced than in the case with L-H_2**L4**, presumably due to the fact that the phenol is protonated and there is less disruption of the electronic structure of the aromatic ring. The structure has one disordered *tert*-butyl group on C(27) which was modeled with partial occupancies of 0.715 and 0.285. A diagram of the full structure is included in the ESI.

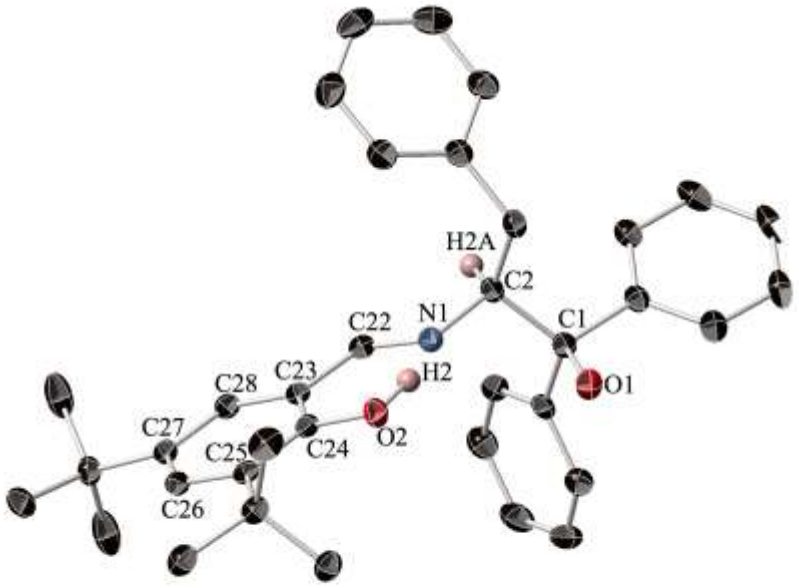

Figure 2. Thermal ellipsoid drawing of L-H_2L6 (hydrogen atoms except H(2) and H(2A) are omitted for clarity; ellipsoids shown at 50% probability). Selected bond distances (Å): C(24)-C(25) 1.405(2), C(25)-C(26) 1.393(2), C(26)-C(27) 1.402(2), C(27)-C(28) 1.385(2), C(23)-C(28) 1.400(2), C(24)-O(2) 1.3570(18), C(1)-O(1) 1.4323(19), C(22)-N(1) 1.278(2).

The molecular structures of L-H_2**L7** and L-H_2**L8** are essentially equivalent to that of L-H_2**L6**, with the expected imine phenol structure. Additional details and complete thermal ellipsoid drawings of all four ligand structures are included in the ESI. Due to the similarity of the ^{1}H NMR spectra between L-H_2L4 and the other ligands, we believe that the iminium-phenoxide tautomer exists only in the solid state, and in solution it exists as the imine-phenol. The C=N bond distance in L-H_2**L4** (1.302(2) Å) is significantly different from that in L-H_2**L6** (1.278(2) Å), L-H_2**L7** (1.274(2) Å) and L-H_2**L8** (1.272(2) Å). However, all five of the ligand C=N stretches are within 11 cm^{-1} of each other. There is no obvious trend in the C=N stretch

between this ligand (1630 cm^{-1}) and either aliphatic substituted L-H_2**L5**/L-H_2**L6** (1625, 1626 cm^{-1}) or fluorinated L-H_2**L7**/L-H_2**L8** (1633, 1636 cm^{-1}) derivatives.

Synthesis and structure of titanium complexes

We next prepared titanium complexes of the ligands starting from $Ti(NMe_2)_4$. All complexes were prepared using the L-enantiomers of the ligands. Ligands H_2**L5** and H_2**L7** had high solubility in ether even at -30 °C, so the synthesis of complexes **10** and **12** were carried out by adding a solution of the ligand to a solution of $Ti(NMe_2)_4$, both in ether at -30 °C (Scheme 3). Upon addition there was an immediate color change from yellow to dark red. Ligands H_2**L4** and H_2**L8** were not soluble in ether at -30 °C so THF was used as the reaction solvent to prepare complexes **9** and **13**, with a similar color change.

The reaction with H_2**L6** was initially carried out in ether, but upon solvent removal, the ^{1}H NMR spectrum showed multiple singlets in the region near 3.5 ppm corresponding to NMe_2 resonances indicating that a clean reaction had not taken place. When the NMR tube containing this mixture was heated at 100 °C overnight, the spectrum simplified and was consistent with the desired product, complex **11**. On a preparative scale, the synthesis of complex **11** was done in toluene in a Teflon-sealed reaction vessel at 100 °C overnight.

After removal of the solvent, all five complexes exhibited clean ^{1}H NMR spectra with two sharp and inequivalent NMe_2 resonances at room temperature. The spectroscopy is consistent with either trigonal bipyramidal or square pyramidal geometry, but titanium,[71] vanadium,[57] and molybdenum[72] complexes with similar ligands all exhibit monomeric distorted square pyramidal structures. The positioning of a strongly π-donating dimethylamide ligand in an axial position would be expected to be favored electronically. The complexes were thermally stable at 100 °C in C_6D_6 solution overnight as evidenced by NMR spectroscopy. Complexes **9,**

11, 12 and **13** were obtained in essentially quantitative yield (85-95%) as dark brown to red oils. The non-quantitative yields are due to spattering during solvent removal; ^{1}H NMR spectroscopy suggests complete conversion to product. Complex **10** was isolated as an orange powder in essentially quantitative yield, but the high solubility of the complex resulted in low yields of 10-25% after recrystallization from ether. The complex has given consistently low combustion analysis results even after multiple recrystallization and analysis attempts. However, the results presented in the experimental section are consistent with theory if an additional oxygen atom is added, presumably due to sample handling. Complex **13** tenaciously retained THF so the observed yield was above 100%, and the solvent is seen in both the ^{1}H and ^{13}C NMR spectra.

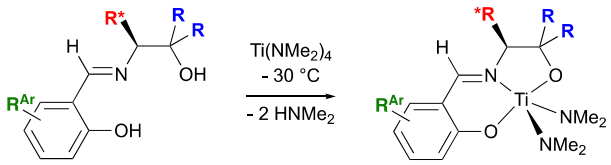

complex	9	10	11	12	13
R	Me	Ph	Ph	Ph	Ph
R*	CH_2Ph	CH_2Ph	CH_2Ph	CH_2Ph	$CHMe_2$
R^{Ar}	H	H	3,5-di-*tert*-butyl	5-F	5-F
ligand	L4	L5	L6	L7	L8
solvent	THF	ether	toluene	ether	THF
yield	84%	96%	93%	96%	100%

Scheme 3. Synthesis of bis-dimethylamide titanium complexes of tridentate iminophenol ligands

In our prior work with amino alcohol ligands, substitution of a dimethylamide group with a chloride often resulted in crystalline complexes. A solution of the ligand H_2**L6** was therefore added to a solution of $TiCl(NMe_2)_3$, both in ether at -30 °C, resulting in an immediate color change from yellow to red followed by precipitation of complex **14** as a yellow powder that was isolated in 75% yield (Scheme 4). This complex exhibits a single sharp NMe_2 resonance in its NMR spectrum. Although the material appeared to be pure by NMR spectroscopy, it needed to

be recrystallized twice from CH_2Cl_2 in order to obtain an analytically pure sample. Like the bis(dimethylamide) complexes **9**-**13**, the NMR spectrum is consistent with either square pyramidal or trigonal bipyramidal geometry. The NMR spectrum of *in situ* prepared D-14 was found to be identical to that of **14**; this spectrum has been included in the ESI.

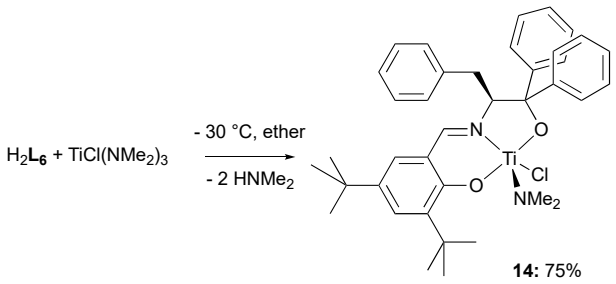

Scheme 4. Synthesis of complex 14

X-ray quality crystals of complex **14** were obtained by crystallization from CH_2Cl_2. A suitable crystal was mounted at 100 K and the structure was determined (Figure 3). The complex exhibits a distorted square pyramidal geometry with the strongly π-donating NMe_2 group on N(2) in an axial position. The atoms in the square plane are the three ligand donors (O(1), O(2) and N(1)) and the chloride. The geometry is characterized with a τ parameter of 0.03.[73] However, the closeness of this value to 0, the value expected for a perfect square pyramid, does not adequately describe how distorted the geometry is. The O-Ti-O and N-Ti-Cl angles are approximately identical at 149.81 and 150.98 ° respectively. The Rc(x) values for the structure is 15.64 for trigonal bipyramidal and 14.84 for square pyramidal, indicating a slightly closer fit to the latter geometry.[74] The distortion from ideal square pyramidal geometry arises from the Ti center being out of the plane defined by O(1), O(2), N(1) and Cl(1) by 0.495 Å.

Complex **14** crystallizes with three molecules of dichloromethane in the lattice. Two of them are disordered over two positions, and the ellipsoids for these molecules are elongated

indicating additional disorder. However, refinement of additional disordered components did not improve the model. A diagram of the full structure, including the solvent molecules, is included in the ESI.

There is not a substantial reorganization of the ligand in complex **14** relative to the structure of H_2**L6** (Figure 2). The benzyl carbon C(7), N(1), and Ti(1) are all almost within the plane described by the aromatic phenol ring. The C-O bond lengths in the complex are both about 0.022 Å shorter than in the free ligand, and the bond alternation seen in the phenoxide ring remains in the titanium complex, suggesting that there is not a significant change to the electronic structure of the ligand upon coordination to titanium.

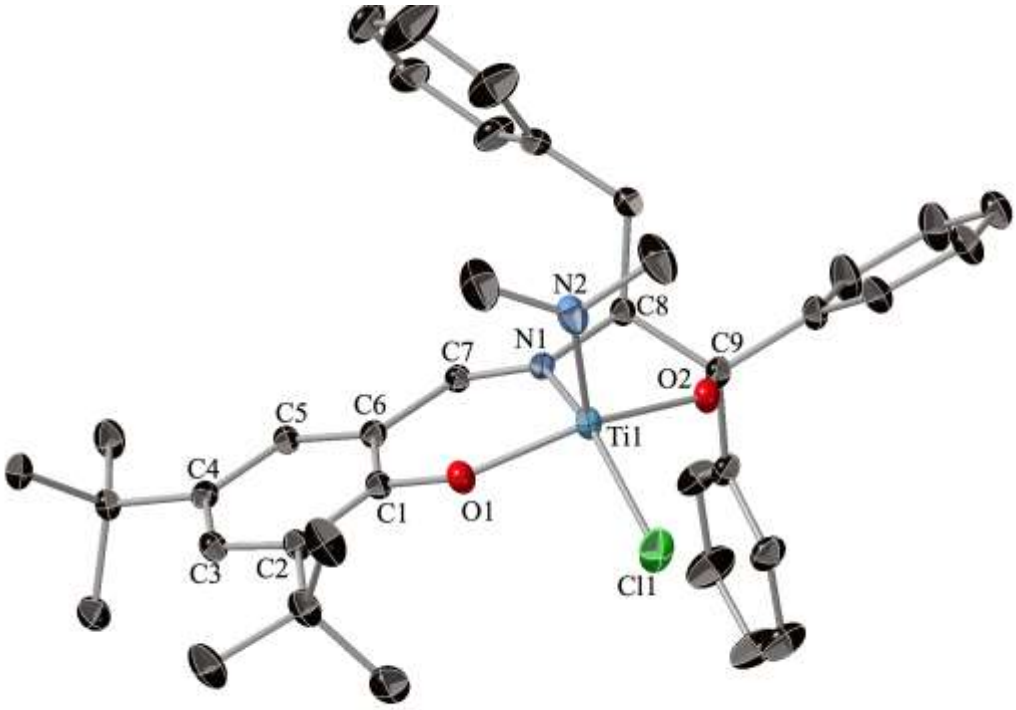

Figure 3. Thermal ellipsoid drawing of complex 14 (three CH_2Cl_2 molecules and all hydrogen atoms are omitted for clarity; ellipsoids shown at 50% probability). Selected bond distances (Å) and angles (°): Ti(1)-Cl(1) 2.3358(8), Ti(1)-O(1) 1.8518(17), Ti(1)-O(2), 1.8424(16), Ti(1)-N(1) 2.1492(18), Ti(1)-N(2) 1.866(2), C(1)-O(1) 1.333(3), C(9)-O(2) 1.411(3), C(1)-C(2) 1.417(3), C(2)-C(3) 1.390(3), C(3)-C(4) 1.409(3), C(4)-C(5) 1.383(3), C(5)-C(6) 1.405(3), C(6)-C(1) 1.410(3), O(2)-Ti(1)-O(1) 149.18(8), O(2)-Ti(1)-N(2) 103.88(9),

O(1)-Ti(1)-N(2) 102.03(9), O(2)-Ti(1)-N(1) 76.03(7), O(1)-Ti(1)-N(1) 81.72(7), N(2)-Ti(1)-N(1) 104.15(9), O(2)-Ti(1)-Cl(1) 94.47(6), O(1)-Ti(1)-Cl(1) 94.81(6), N(2)-Ti(1)-Cl(1) 104.74(8), N(1)-Ti(1)-Cl(1) 150.99(6).

Tridentate imine diol ligands identical or similar to those reported here have been used in a variety of metal mediated transformations, as well as structural[71, 75] and synthetic studies. Copper complexes of **L6** and related ligands,[72, 76-79] and the vanadium[57] and molybdenum[72] complexes of **L6** have also been reported. The titanium chloride complex is essentially isostructural to V(O)(**L6**)(OEt), which has the strongly π-donating oxo ligand in the axial position, and $Mo(O)_2$(**L6**), which has oxo ligands in both the axial and equatorial positions. The V structure is more distorted than the Ti structure, with a τ parameter of 0.44 and an Rc(x) of 17.00, while the Mo structure has a τ parameter of 0 and an Rc(x) of 15.80 (both favoring a distorted square bipyramid). A more closely related structure is the pseudooctahedral 2:1 complex of Ti with a closely related XLX ligand prepared from 2 equivalents of ligand and $Ti(O^iPr)_4$. The Ti-O and Ti-N bond lengths in that complex correspond closely to those for complex **14**, with slightly longer Ti-OAr bonds of 1.938(4) and 1.912(4) Å; the Ti-OR bond lengths are 1.835(4) and 1.882(4) Å.[71]

Intramolecular hydroamination of aminoallenes

Hydroamination was carried out using our previously described *in situ* procedures.[41, 43] We have not observed significant differences in either catalytic activity or enantioselectivity using this method as compared to using isolated complexes as catalysis.[43] We prepared titanium precatalyst complexes *in situ* by mixing stock solutions of the desired ligand with $Ti(NMe_2)_4$ in benzene-d_6 in a J. Young NMR tube. Catalysis was initiated by adding a stock solution of the aminoallene substrate in benzene-d_6 followed by heating to either 110 °C (substrate **1a**) or 135

°C (substrate **1a** and **1b**). Reactions were monitored periodically by ^{1}H NMR spectroscopy and were quenched when complete or when no further progress was observed after 24 hours. Unlike our prior results with these substrates, we were unable to achieve 100% conversion. Run-to-run repeatability of enantioselectivity values is ±2% ee, which is also approximately the error with repeat injections of the same sample. We did not test the monochloride complexes of the ligands for catalytic activity. In the past, we have found that chloride substituents shut down the reaction,[53] as has been observed by others.[80]

The catalytic hydroamination of hepta-4,5-dienylamine (**1a**) gave all three possible products as observed by NMR spectroscopy.[81] Unlike our previously reported bidentate aminoalcohol ligands, where the *Z*- and *E*-5-exo pyrrolidine products (**3a**) were favored over the tetrahydropyridine (**2a**) with regioselectivities ranging from 2-4:1, we observed a lower selectivity around 1:1 (Table 2). The product ratios were determined by comparison with known spectra.[81] The *Z*/*E* ratio for the 5-exo product is relatively low, ranging from 1.3:1 for complex **9** (entry 1) to almost 3:1 for entry the two fluorinated complexes **12** and **13** (entries 4 and 5). Catalytic reactions were carried out at 135 °C for this substrate. The reaction reached 86-97% completion before stalling. Enantioselectivities were determined by conversion of the pyrrolidine to the benzyl derivative using benzyl bromide, followed by separation and analysis by chiral GC-MS. The *Z*- and *E*-pyrrolidine products were obtained in a maximum of 8-10 %ee with complex **9** (entry 1). Complex **11** gave the highest yield of the undesired tetrahydropyridine (entry 3). This result suggests that increased steric bulk of the ligand favors the addition to the external double bond of the substrate (C5-C6) relative to the internal double bond (C4-C5).

Table 2. Hydroamination of hepta-4,5-dienylamine at 135 °C with *in situ* catalysts (5 mol% catalyst) to give tetrahydropyridine 2a, *Z*- or *E*-α-vinylpyrrolidines *Z*- and *E*-3a

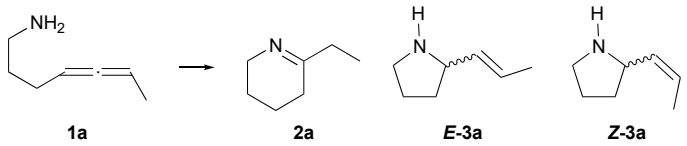

1a 2a *E*-3a *Z*-3a

				Yield (%)[a]		
Entry	Complex	*t*/h	% conv.	**2a**	*E*-**3a** (ee[b])	Z-**3a** (ee[b])
1	**9**	43	76	46	17 (9%)	22 (8%)
2	**10**	31	87	40	14 (1%)	36 (2%)
3	**11**	54	96	72	8 (3%)[c]	17 (7%)
4	**12**	54	91	44	13 (2%)[c]	38 (1%)
5	**13**	54	88	42	13 (2%)[c]	39 (2%)

[a]Relative amount of imine:5-exo determined by NMR, ±2%. [b]Of the benzyl derivative, determined by GC, ±2%. [c]Enantiomer with shorter R_f favored. Data reported as the average of two individual runs.

With 6-methyl-hepta-4,5-dienylamine, hydroamination was carried out at 135 °C and gave exclusively 2-(2-methylpropenyl)pyrrolidine (**3b**) (Table 3). The reaction stopped typically after 75-80% conversion within 48 hours, though in some cases, the reaction continued for up to 90 hours. Complex **9** gave essentially no conversion to product even after nearly 70 hours (entry 1). Enantioselectivity was again determined by chiral GC-MS of the benzyl derivative. Both the *N*-benzyl and the *N*-tosyl derivative of this product is known.[43, 82] In the past, ligand sterics have corresponded with higher enantioselectivity for hydroamination of this substrate,[42, 43] and this trend continues here. The highest enantioselectivity we observed was 17 %ee with complex **11** (entry 3). This value is within error of the highest reported enantioselectivity for this substrate with a Ti catalyst,[42] but is lower than our reported Ta catalyzed reaction with bidentate aminoalcohol ligands.[43] We next carried out the hydroamination reaction using D-H_2**L6** to generate complex D-**11** *in situ*. In the past, we have observed equal and opposite enantioselectivity within error for the hydroamination reaction when using the D-enantiomers of the ligands as catalysts. Surprisingly, the reaction with D-**11** took place with no enantioselectivity

(entry 6) even after multiple repeat runs and ensuring that the ligand was obtained in high optical purity by polarimetry. We are continuing to investigate this unexpected result that suggests that our catalysts derived from tridentate X_2L complexes are not simply enantiomers of one another.

Table 3. Hydroamination of 6-methyl-hepta-4,5-dienylamine 1c at 135 °C with *in situ* catalysts (5 mol% catalyst).

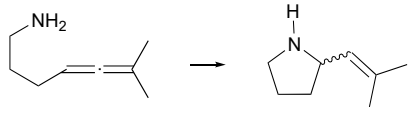

1b **3b**

41.3, 42.1 min

Entry	Complex	*t*/h	% conv.	%ee[a]	Config[b]
1	**9**	67	7	11	S-(-)
2	**10**	43	86	6	S-(-)
3	**11**	34	87	17	S-(-)
4	**12**	81	73	1	S-(-)
5	**13**	65	74	3	S-(-)
6	**D-11**	16	95	0	-

[a]Of the benzyl derivative, determined by GC, ±2%. [b]Determined by comparison to literature values.[43, 83-85] Data reported as the average of two individual runs.

Conclusion

The evidence from our prior work suggested that monomeric Ti complexes would be better hydroamination catalysts than the dimeric ones we have used previously with bidentate amino alcohol derived ligands. Incorporation of a dative coordinating atom into a tridentate ligand scaffold allowed us to explore this hypothesis. We prepared five tridentate iminophenol ligands and obtained the crystal structures of four of them. The ligands exhibit hydrogen bonding networks that in one case causes a tautomerization to the iminium phenoxide structure in the solid state. For one ligand, we prepared the titanium complex starting from $TiCl(NMe_2)_3$ and obtained its crystal structure. The complex was monomeric, exhibiting a distorted square pyramidal geometry. We prepared their titanium complexes starting from $Ti(NMe_2)_4$, and while

they were pure by NMR spectroscopy, they were for the most part intractable oils. We used these complexes as *in situ* catalysts for the intramolecular hydroamination of two aminoallene substrates. One catalyst gave slightly higher enantioselectivity than the catalysts derived from our bidentate amino alcohol ligands. In the case of the 6-methyl-hepta-4,5-dienylamine substrate, increased sterics of the ligand does seem to improve enantioselectivity without a detrimental decrease in conversion to product. Further studies in this ligand design will be focused on increasing the steric environment at the 3-position of the phenol ring in order to test this hypothesis.

Conflicts of Interest

There are no conflicts of interest to declare.

Acknowledgements

Financial support for this project was received from the National Science Foundation, NSF-MRI-1725142, the John Stauffer Fund for Summer Research in Chemistry, the Harvey Mudd College Chemistry Department, the Thomas Poon Endowed Internship Fund, and the Dean of the Faculty at Pitzer College.

Experimental

General

All reagents were obtained from commercial suppliers and were purified by standard methods[86] or used as received. Ligand precursors (*S*)-2-amino-1,1,3-triphenylpropanol,[62, 63] (*S*)-2-amino-3-phenyl-l,1-dimethylpropanol[64] and (S)-2-amino-3-methyl-1,1-diphenylbutanol[62] were prepared by literature procedures. L-H_2**L5** and L-H_2**L6** have been prepared previously, though by slightly different procedures.[57, 87] The purity of compounds was established by ^{1}H NMR

spectroscopy and elemental analysis. Solvents were purified by vacuum transfer from sodium/benzophenone (C_6D_6) or by passage through a column of activated alumina (Innovative Technology PS-400-5-MD) and stored under nitrogen (diethyl ether, tetrahydrofuran, dichloromethane, hexane, and toluene). Solutions of ligands (ca. 0.05 M in C_6D_6) and substrates (ca. 1.5 M in C_6D_6) for catalysis were dried over molecular sieves overnight and stored at -35 °C. All air and/or moisture sensitive compounds were manipulated under an atmosphere of nitrogen using standard Schlenk techniques, or in a glovebox (MBraun Unilab). ^{1}H and ^{13}C NMR spectra were recorded at ambient temperature on a Brüker Avance NEO 400 spectrometer and referenced to internal tetramethylsilane or residual solvent peaks. Carbon assignments were made using DEPT experiments. J values are given in Hz. Polarimetry was carried out using a JASCO P1010 instrument. IR spectroscopy was carried out using a Thermo-Nicolet iS5 FTIR using a diamond anvil ATR accessory. GC-MS analysis was carried out using a Hewlett Packard 5890 Series II Gas Chromatograph. Mass spectra were obtained using an Advion expression^{L} APCI Mass Spectrometer with quadrupole mass analyzer. Specific rotation values $[\alpha]_D$, are given in 10^{-1} deg cm^2 g^{-1}. Elemental analyses were performed by ALS Global, Tucson, AZ or Midwest Microlab, Indianapolis, IN.

2-hydroxy-benzaldehyde 3*S*-(2-methyl-4-phenylpropan-2-ol) imine (L-H_2L4)

L-2-Amino-l,1-dimethyl-3-phenylpropanol (1.2459 g, 6.95 mmol) and salicylaldehyde (0.74 mL, 6.9 mmol) were each dissolved in hot ethanol (~35 mL, 0.2 M). The salicylaldehyde solution was added slowly to the amine, and the reaction immediately turned bright yellow. The reaction was heated at reflux for 3 hours before being allowed to cool to room temperature and stir overnight. The reaction mixture was concentrated under reduced pressure to yield crude product. The crude product was recrystallized from a minimum of hot ethanol to yield a bright

yellow solid (1.0930 g, 3.86 mmol, 56%). Mp: 159.6-162.2 °C. $[\alpha]_D$ (c = 0.0116 g·mL^{-1}, EtOAc): -329°. Anal. Calcd for $C_{18}H_{21}NO_2$: C, 76.3; H, 7.47; N, 4.94. Found: C, 75.98; H, 7.51; N, 5.00. IR: 1630 (CN). ^{1}H NMR (400 MHz, $CDCl_3$):δ 7.68 (s, 1H, imine), 7.31-6.80 (m, 9H, ArH), 3.23 (dd, 1H, *J* = 2, 13, C*H*CH_aH_bPh), 3.18 (dd, 1H, *J* = 2, 10, $CHCH_a$*H*$_b$Ph), 2.79 (dd, 1H, *J* = 11, 13, CHC*H*$_a$$H_b$Ph), 1.66, (br s, 1H, OH), 1.43 (s, 3H, C*H*$_{3a}$), 1.38 (s, 3H, C*H*$_{3b}$). ^{13}C NMR (100 MHz, $CDCl_3$): δ 166.37 (C=N), 161.30 (4°), 139.15 (4°), 132.72 (CH), 131.82 (CH), 129.96 (CH), 128.69 (CH), 126.59 (CH), 118.97 (CH), 118.71 (4°), 117.18 (CH), 81.94 (Me_2*C*OH), 72.79 (CHN), 37.98 (CH_2), 26.84 (CH_3), 26.46 (CH_3). MS (APCI): *m/z* 284.3 ($[M+H]^+$, 100%). IR (ATR, diamond): ν_{CN} = 1630 cm^{-1}.

2-Hydroxy-benzaldehyde 3*R*-(2-methyl-4-phenylpropan-2-ol) imine (D-H$_2$L4)

D-2-Amino-l,1-dimethyl-3-phenylpropanol (0.2825 g, 1.58 mmol) and salicylaldehyde (0.168 mL, 1.58 mmol) were each dissolved in hot ethanol (~15 mL, 0.1 M). The salicylaldehyde solution was added slowly to the amine, and the reaction immediately turned bright yellow. The reaction was heated at reflux for 3 hours before being allowed to cool to room temperature and stir overnight. The reaction mixture was concentrated under reduced pressure to yield crude product. The crude product was recrystallized from a minimum of ethanol yielding a bright yellow solid (0.2865 g, 1.01 mmol, 64%). The ^{1}H NMR spectrum matched that of the L-enantiomer. $[\alpha]_D$ (c = 0.0104 g·mL^{-1}, EtOAc): +325°. Anal. Calcd for $C_{18}H_{21}NO_2$: C, 76.3; H, 7.47; N, 4.94. Found: C, 76.21; H, 7.48; N, 4.93.

2-Hydroxy-benzaldehyde 2*S*-(1,1,3-triphenylpropanol) imine (L-H$_2$L5)

L-2-Amino-1,1,3-triphenylpropanol (1.0237g, 3.37 mmol) and salicylaldehyde (0.36 mL, 3.37 mmol) were each dissolved in hot ethanol (~30 mL, 0.1 M). The aldehyde solution was

added slowly to the amine, and the reaction immediately turned bright yellow. The reaction was heated at reflux for 3 hours then allowed to cool to room temperature and stir overnight. The reaction mixture was concentrated under reduced pressure to yield crude product. The crude product was recrystallized from ethanol to yield a yellow solid (0.8532 g, 2.09 mmol, 62%). The ^{1}H NMR spectrum was consistent with the literature data.[57] Mp: 153.4-161.5 °C. $[\alpha]_D$ (*c* = 0.0092 g·mL^{-1}, EtOAc): -156°. IR: 1614 (CN). ^{1}H NMR (400 MHz, $CDCl_3$): δ 7.65-6.75 (m, 19 H), 7.57 (s, 1H, *H*C=N), 4.35 (dd, 1H, *J* = 2, 10, C*H*CH_aH_bPh), 3.04 (dd, 1H, *J* = 2, 14, $CHCH_a$*H*$_b$Ph), 2.92 (s, 1H, OH), 2.84 (dd, 1H, *J* = 10, 14, CHC*H*$_a$$H_b$Ph). MS (APCI): *m/z* 408.4 ($[M+H]^+$, 100%). IR (ATR, diamond): ν_{CN} = 1626 cm^{-1}.

2-Hydroxy-benzaldehyde 2*R*-(1,1,3-triphenylpropanol) imine (D-H_2L5)

D-2-Amino-1,1,3-triphenylpropanol (0.5099 g, 1.65 mmol) and salicylaldehyde (0.175 mL, 1.64 mmol) were each dissolved in hot ethanol (~14 mL, 0.1 M). The aldehyde solution was added slowly to the amine, and the reaction immediately turned bright yellow. The reaction was heated at reflux for 3 hours then allowed to cool to room temperature and stir overnight. The reaction mixture was concentrated under reduced pressure to yield crude product. The crude product was recrystallized from hexane:toluene to yield a yellow solid (0.4046 g, 0.993 mmol, 61%). The ^{1}H NMR spectrum matched that of the L-enantiomer. $[\alpha]_D$ (*c* = 0.0107 g·mL^{-1}, EtOAc): +173°.

2-Hydroxy-3,5-di-*tert*-butyl-benzaldehyde 2*S*-(1,1,3-triphenylpropanol) imine (L-H_2L6)

L-2-amino-1,1,3-triphenylpropanol (0.6527 g, 2.15 mmol) and 3,5-di-*tert*-butylsalicylaldehyde (0.5040 g, 2.15 mmol) were each dissolved in hot ethanol (~20 mL, 0.1 M). The salicylaldehyde solution was added slowly to the amine, and the reaction immediately turned

bright yellow. The reaction was heated at reflux overnight. The reaction mixture was concentrated under reduced pressure to a yield a bright yellow foam (1.0466 g, 2.01 mmol, 93%). The ^{1}H and ^{13}C NMR spectra was consistent with those previously reported, though the imine proton was not identified and the coupling constant for the benzylic hydrogens in the original report were incorrect.[57] The compound could be purified to remove residual aldehyde, if present, by recrystallization from ethanol (35% recovery) or column chromatography (hexane/ethyl acetate, 42% recovery). Mp: 148.6-151.2 °C. $[\alpha]_D$ (*c* = 0.00672 g·mL^{-1}, EtOAc): -155°. IR: 1625 (CN). ^{1}H NMR (400 MHz, $CDCl_3$): δ 12.83 (br s, OH), 7.62 (s, 1H, *H*C=N), 7.49-6.66 (m, 17H), 4.35 (dd, 1H, *J* = 2, 10, C*H*CH_aH_bPh), 3.01 (br s, 1H, OH), 3.007 (dd, 1H, *J* = 2, 14, $CHCH_a$*H*$_b$Ph), 2.86 (dd, 1H, *J* = 10, 14, $CHCH_a$*H*$_b$Ph), 1.40 (s, 9H, ^{t}Bu), 1.22 (s, 9H, ^{t}Bu). MS (APCI): *m/z* 520.6 ($[M+H]^+$, 100%). IR (ATR, diamond): ν_{CN} = 1625 cm^{-1}.

2-Hydroxy-3,5-di-*tert*-butyl-benzaldehyde 2*R*-(1,1,3-triphenylpropanol) imine (D-H_2L6)

D-2-Amino-1,1,3-triphenylpropanol (0.367 g, 1.21 mmol) and 3,5- di-*tert*-butylsalicylaldehyde (0.2551 g, 1.09 mmol, 0.9 equiv.) were each dissolved in hot ethanol (~10 mL, 0.1 M). The salicylaldehyde solution was added slowly to the amine, and the reaction immediately turned bright yellow. The reaction was heated at reflux overnight. The reaction mixture was concentrated under reduced pressure to a yield a yellow product (0.5682 g, 1.09 mmol, 100%). The compound was purified by recrystallization from methanol (42% recovery). The ^{1}H spectrum matched that of the L-enantiomer. $[\alpha]_D$ (*c* = 0.00684 g·mL^{-1}, EtOAc): +159°.

2-Hydroxy-5-fluoro-benzaldehyde 2*S*-(1,1,3-triphenylpropanol) imine (L-H_2L7)

L-2-Amino-1,1,3-triphenylpropanol (0.2938 g, 0.97 mmol) and 5-fluorosalicylaldehyde (0.1357 g, 0.97 mmol) were each dissolved in hot ethanol (~10 mL, 0.1 M). The salicylaldehyde

solution was added slowly to the amine, and the reaction immediately turned bright yellow. The reaction was heated at reflux for 4 hours then allowed to cool to room temperature and stir overnight. The reaction mixture was concentrated under reduced pressure to a yield a bright yellow solid (0.3859, 0.91 mmol, 94%). The compound could be purified by recrystallization from toluene/hexane (60% recovery). Mp: 147.7 - 150.1 °C. $[\alpha]_D$ (c = 0.00636 g·mL^{-1}, EtOAc): -164°. Anal. Calcd: C, 79.04; H, 5.69; N, 3.29. Found: C, 79.06; H, 5.92; N, 3.36. IR: 1633 (CN). ^{1}H NMR (400 MHz, $CDCl_3$): δ 12.43 (s, 1H, OH), δ 7.64-6.53 (m, 18H), 7.48 (s, 1H, *H*C=N), 4.35 (dd, 1H, J = 10, 2, C*H*CH$_a$H$_b$Ph), 3.06 (dd, 1H, J =14, 2, CHC*H$_a$*H$_b$Ph), 2.89 (br s, 1H, OH), 2.83 (dd, 1H, J = 10, 14, CHCH$_a$*H$_b$*Ph). ^{13}C NMR (100 MHz, $CDCl_3$): δ 165.74 (d, J_{CF} = 3, CN), 156.94 (4°), 154.44 (d, J_{CF} = 235 Hz, CF), 145.52 (4°), 144.26 (4°), 139.03 (4°), 130.04 (CH), 128.85 (CH), 128.75 (CH), 128.67 (CH), 127.55 (CH), 127.40 (CH), 126.81 (CH), 126.50 (CH), 126.34 (CH), 119.76 (d, J_{CF} = 23, *C*H ortho to CF), 118.37 (*C*CH=N), 118.11 (d, J_{CF} = 7, CH), 116.85 (d, J_{CF} = 23 Hz, *C*H ortho to CF), 80.06 (*C*Ph$_2$OH), 79.15 (CHN), 37.69 (CH_2). MS (APCI): *m/z* 426.4 ([M+H]$^+$, 100%). IR (ATR, diamond): ν_{CN} = 1633 cm^{-1}.

2-Hydroxy-5-fluoro-benzaldehyde 2*R*-(1,1,3-triphenylpropanol) imine (D-H$_2$L7)

D-2-amino-1,1,3-triphenylpropanol (0.673 g, 2.22 mmol) and 5-fluorosalicylaldehyde (0.311 g, 2.22 mmol) were each dissolved in hot ethanol (~20 mL, 0.1 M). The salicylaldehyde solution was added slowly to the amine, and the reaction immediately turned bright yellow. The reaction was heated at reflux for 4 hours then allowed to cool to room temperature and stir overnight. The reaction mixture was concentrated under reduced pressure to a yield a yellow oil and was purified by column chromatography (hexane, ethyl acetate ramp) to yield a crystalline solid (0.367 g, 0.863 mmol, 39%). The ^{1}H NMR was consistent with that of the L-enantiomer. $[\alpha]_D$ (c = 0.00584 g·mL^{-1}, EtOAc): +163°.

2-Hydroxy-5-fluoro benzaldehyde 2*S*-(2-amino-3-methyl-1,1-diphenylbutanol) imine (L-H_2L8)

(*S*)-2-Amino-3-methyl-1,1-diphenylbutanol (1.2252 g, 4.80 mmol) and 5-fluorosalicylaldehyde (0.6722 g, 4.80 mmol) were each dissolved in hot ethanol (~20 mL, 0.25 M). The salicylaldehyde solution was added slowly to the amine, and the reaction immediately turned bright yellow. The reaction was heated at reflux for 3 hours then allowed to cool to room temperature and stir overnight. The reaction mixture was concentrated under reduced pressure to yield a bright yellow solid (1.6817 g, 4.46 mmol, 93%). The compound was purified by vapor diffusion of hexane into a toluene solution (35 % recovery). Mp: 193.8 - 194.6 °C. $[\alpha]_D$ (*c* = 0.00500 g·mL^{-1}, EtOAc): +47.4°. Anal. Calcd: C, 76.37; H, 6.41; N, 3.71. Found: C, 76.15; H, 6.47; N, 3.82. IR: 1636 (CN). ^{1}H NMR (400 MHz, $CDCl_3$): δ 12.70 (s, 1H, OH), δ 8.10 (s, 1H, *H*CN), 7.61-6.87 (m, 13H), 4.05 (d, 1H, *J* = 2, C*H*CHMe$_2$), 2.78 (s, 1H, OH), 2.17 (dsept, 1H, *J* = 2, 7, CHC*H*Me$_2$), 0.97 (d, 3H, *J* = 7, *Me$_a$*Me$_b$CH), 0.82 (d, 3H, *J* = 7, Me$_a$*Me$_b$*CH). ^{13}C NMR (100 MHz, $CDCl_3$): δ 165.92 (d, J_{CF} = 3, C=N), 157.26 (d, J_{CF} = 1, 4°), 155.9 (d, J_{CF} = 276, CF), 146.26 (4°), 144.51 (4°), 128.64 (CH), 128.60 (CH), 127.24 (CH), 127.18 (CH) 126.21 (CH), 126.13(CH), 119.95 (d, J_{CF} = 23, *C*H ortho to CF), 118.54 (d, J_{CF} = 7, *C*CH=N), 118.30 (d, J_{CF} = 7, CH), 116.97 (d, J_{CF} = 23, *C*H ortho to CF), 80.95 (CN), 77.56 (*C*Ph$_2$OH), 29.28 (*C*HMe$_2$), 22.90 (CH_3), 18.29 (CH_3). MS (APCI): *m/z* 378.4 ([M+H]$^+$, 100%). IR (ATR, diamond): ν_{CN} = 1636 cm^{-1}.

2-Hydroxy-5-fluoro benzaldehyde 2*R*-(2-amino-3-methyl-1,1-diphenylbutanol) imine (D-H_2L8)

(*R*)-2-Amino-3-methyl-1,1-diphenylbutanol (0.3063 g, 1.2 mmol) and 5-fluorosalicylaldehyde (0.1681 g, 1.2 mmol) were each dissolved in hot ethanol (~15 mL, 0.1 M).

The salicylaldehyde solution was added slowly to the amine, and the reaction immediately turned bright yellow. The reaction was heated at reflux for 3 hours then allowed to cool to room temperature and stir overnight. The reaction mixture was concentrated under reduced pressure to yield a bright yellow solid, which was then recrystallized from toluene and hexanes (0.2195 g, 0.582 mmol, 49%). The ^{1}H NMR was consistent with that of the L-enantiomer. $[\alpha]_D$ (*c* = 0.00488 g·mL^{-1}, EtOAc): -52.4°.

Complex L-9, Ti(L-L4)(NMe$_2$)$_2$

L-H$_2$**L4** (0.149 g, 0.526 mmol) and Ti(NMe$_2$)$_4$ (0.118 g, 0.526 mmol) were each dissolved in THF (3 mL) and cooled to -30 °C. The ligand solution was added to the metal solution causing a rapid color change to red/orange. The reaction was stirred for 25 hours before the solvent was removed to yield a dark brown thick oil (0.263 g, 0.440 mmol, 84%). ^{1}H NMR (400 MHz, C_6D_6): δ = 7.12-7.15 (m, 2 H), 6.89-7.01 (m, 3H), 6.86 (s, 1H, NC=H), 6.672 (m, 2H), 6.52-6.54 (m, 2H), 3.62 (s, 6H, NMe$_2$), 3.57 (s, 6H, NMe$_2$), 3.24 (dd, 1H, J = 3, 11, C*H*CH$_a$H$_b$Ph), 2.98 (dd, 1H, J = 3, 13, CHC*H$_a$*H$_b$Ph), 2.87 (dd, 1H J = 11, 13, CHCH$_a$*H$_b$*Ph), 1.30 (s, 3H, CH$_3$), 1.28 (s, 3H, CH$_3$). ^{13}C NMR (100 MHz, C_6D_6): δ = 165.35 (N=CH), 164.76 (4°, PhO), 139.16 (4°), 135.51 (CH), 133.84 (CH), 131.22 (CH), 129.06 (CH), 121.96 (4°), 121.11 (CH), 120.04 (CH), 118.41 (CH), 85.84 (4°), 83.00 (CH), 49.89 (N(CH$_3$)$_2$), 49.61 (N(CH$_3$)$_2$), 38.71 (CH$_2$), 32.67 (CH$_3$), 26.79 (CH$_3$).

Complex L-10, Ti(L-L5)(NMe$_2$)$_2$

L-H$_2$**L5** (0.147 g, 0.36 mmol) was dissolved in ether (10 mL) and Ti(NMe$_2$)$_4$ (0.081 g, 0.36 mmol) was dissolved in ether (3 mL) and both solutions were cooled to -30 °C. The ligand solution was added to the metal solution causing a color change from yellow to ruby red. After 24 hours, the solvent was removed to give an orange powder (0.188 g, 0.347 mmol, 96%). The

compound crystallized from ether in low yield (ca. 20-50 mg, 10-25%) to give orange microcrystals. The best combustion analysis data we have obtained for this complex is consistent with an additional oxygen atom. M.p. 155.7-159.1 °C. Anal. Calcd for $C_{32}H_{35}N_3O_2Ti$: C, 70.98; H, 6.52; N, 7.76. Calcd for $C_{32}H_{35}N_3O_3Ti$: C, 68.94, H, 6.33; N, 7.54. Found: C, 69.06; H, 5.90; N, 7.16. ^{1}H NMR (400 MHz, C_6D_6): δ 7.88 (br d, 2H, *J* = 7 Hz), 7.53 (br d, 2H, *J* = 8 Hz), 7.31 (br t, 2H, *J* = 7 Hz), 7.22 (s, 1H, *H*CN), 6.77-7.11 (Ph*H* m, 11 H), 6.56 (dd, 1H, *J* = 2, 8 Hz, ArH), 6.48 (dd, 1H, *J* = 1, 8 Hz, ArH), 4.68 (t, 1H, *J* = 7 Hz, C*H*CH_2Ph), 3.57 (s, 6H, NMe_2), 3.46 (s, 6H, NMe_2), 2.92 (d, 2H, *J* = 7 Hz, CHC*H*$_2$Ph). ^{13}C NMR (100 MHz, C_6D_6): δ 165.30 (H*C*=N), 164.22 (*Ph*-O), 149.97 (4°), 148.05 (4°), 139.61 (4°), 135.59 (CH), 133.77 (CH), 131.22 (CH), 129.23 (CH), 129.10 (CH), 128.87 (CH), 127.54 (CH), 127.31 (CH), 127.26 (CH), 127.18 (CH), 127.15 (CH), 121.95 (CH), 119.87 (CH), 119.00 (*C*CH=N), 90.85 (*C*Ph_2OR), 84.34 (C-N), 49.21 (Me_2), 48.24 (Me_2), 39.66 (CH_2Ph).

Complex L-11, Ti(L-L6)(NMe_2)$_2$

L-H_2**L6** (0.231 g, 0.446 mmol) and Ti(NMe_2)$_4$ (0.100 g, 0.446 mmol) were each dissolved in toluene (3 mL) and cooled to -30 °C. The ligand solution was added to the metal solution causing a color change from yellow to ruby red. The solution was transferred to a Teflon-valved glass reaction vessel and heated at 100 °C overnight. Removal of the solvent yielded a dark red-brown foam (0.272 g, 0.416 mmol, 93% yield). ^{1}H NMR (400 MHz, C_6D_6): δ 6.6-7.8 (m, 17H), 4.73 (dd, J = 2, 11, C*H*CH_aH_bPh), 3.51 (s, 6H, (NMe_2)), 3.33 (s, 6H, (NMe_2)), 2.84 (dd, J = 2, 13, CHC*H*$_a$H$_b$Ph), 2.73 (dd, 1H, J = 11, 13, CHCH$_a$*H*$_b$Ph), 1.58 (s, 9H, 3-^{t}Bu), 1.23 (s, 9H, 5-^{t}Bu). ^{13}C NMR (100 MHz, C_6D_6): δ 166.43 (C=N), 161.92 (Ph-O), 150.53 (4°), 148.84 (4°), 140.58 (tBu*C*), 140.04 (*Ph*CH_2R), 139.29 (tBu*C*), 131.21 (CH), 130.61 (CH), 129.15* (two CH resonances), 128.88 (CH), 128.33 (CH), 127.83 (CH), 127.33 (CH), 127.18

(CH), 127.16 (CH), 127.06 (CH), 121.69 (*C*HCO), 90.81 (*C*Ph_2OR), 83.20 (C-N), 47.6 (Me_2), 48.51 (Me_2), 46.77 (CH_2), 36.18 (*C*Me_3), 34.77 (*C*Me_3), 32.12 (Me_3), 30.60 (Me_3). One CH in the aromatic region was not located but the peak at 129.15 is larger than the others.

Complex L-12, Ti(L-L7)(NMe_2)$_2$

L-H_2**L7** (0.190 g, 0.446 mmol) and Ti(NMe_2)$_4$ (0.100 g, 0.446 mmol) were each dissolved in ether (ca. 5 mL) and cooled to -30 °C. The ligand solution was added to the metal solution and there was a color change from yellow to dark red. Removal of the solvent yielded a dark red oil (0.24 g, 0.429 mmol, 96% yield). ^{1}H NMR (400 MHz, C_6D_6): δ 6.19-7.87 (m, 19H), 4.63 (dd, 1H, *J* = 5, 9, C*H*CH_2Ph), 3.53 (s, 6H, (NMe_2)), 3.45 (s, 6H, (NMe_2)), 2.90 (m, 2H, CHC*H*$_2$Ph). ^{13}C NMR (100 MHz, C_6D_6): δ 164.31 (d, J_{CF} = 3, C=N), 160.48 (Ph-O), 155.80 (d, J_{CF} = 235, CF), 149.88 (4°), 147.86 (4°), 139.39 (4°), 131.11 (CH), 129.27 (CH), 129.14 (CH), 128.92 (CH), 127.46 (CH), 127.39 (CH), 127.38 (CH), 127.31 (CH), 127.08 (CH), 122.87 (d, J_{CF} = 23, *C*HCF), 121.25 (d, J_{CF} = 8 Hz, *C*CH=N), 120.88 (d, J_{CF} = 7, *C*HCO), 117.77 (d, J_{CF} = 23, *C*HCF), 90.93 (*C*Ph_2O), 84.40 (C-N), 49.15 (CH_3), 48.18 (CH_3), 39.55 (CH_2).

Complex L-13, Ti(L-L8)(NMe_2)$_2$

L-H_2**L8** (0.168 g, 0.446 mmol) and Ti(NMe_2)$_4$ (0.100 g, 0.446 mmol) were each dissolved in THF (ca. 5 mL) and cooled to -30 °C. The ligand solution was added to the metal solution and there was a color change from yellow to dark red. Removal of the solvent yielded a dark orange oil that tenaciously retained THF (0.247 g, >100%). ^{1}H NMR (400 MHz, C_6D_6): δ 7.80 (s, 1H, imine), 6.68-7.79 (m, 13H), 4.28 (d, 1H, *J* = 5 Hz, C*H*CHMe_2), 3.53 (s, 6H, (NMe_2)), 3.15 (s, 6H, (NMe_2)), 2.16 (m, 1H, CHC*H*Me_2), 0.60 (d, 3H, *J*= 7, CH_3), 0.43 (d, 3H, J = 7, CH_3). ^{13}C NMR (100 MHz, C_6D_6): δ 164.27 (d, J_{CF} = 3, C=N), 160.99 (Ph-O), 156.78 (d, J_{CF} = 235, CF), 150.58 (4°), 147.44 (4°), 128.90 (CH), 128.93 (CH), 128.65 (CH), 127.97 (CH), 127.30 (CH),

127.14 (CH), 123.13 (d, J_{CF} = 23, *C*HCF), 121.29 (d, J_{CF} = 7, *C*HC-O), 121.19 (d, J_{CF} = 8, *C*CH=N), 118.13 (d, J_{CF} = 23, *C*HCF), 90.41 (*C*Ph_2O), 86.44 (C-N), 48.86 (CH_3), 47.75 (CH_3), 30.69 (*C*Me_2H), 22.92 (CH_3), 20.00 (CH_3).

Complex L-14, Ti(L-L6)(NMe_2)Cl

L-H_2**L6** (0.245 g, 0.47 mmol, 1 eq.) and $TiCl(NMe_2)_3$ (0.102 g, 0.47 mmol, 1 eq) were dissolved separately in ether (5 mL) and cooled at -35 °C for 15 minutes. The ligand was added dropwise to the metal reagent with stirring. There was an immediate color change from yellow to red and within minutes a yellow solid precipitated from solution. The reaction was allowed to warm to room temperature and stir overnight. The solid was isolated via vacuum filtration to yield a light yellow powder (0.229 g, 0.35 mmol, 75% yield). The material could be recrystallized from CH_2Cl_2 to obtain analytically pure material. Mp: 183.6-189.4 °C. Anal. Calcd: C, 70.65; H, 7.03; N, 4.34. Found: C, 70.27; H, 6.98; N, 4.51 . ^{1}H NMR (400 MHz, C_6D_6): δ 7.9 (m, 4H), (7.58, d, 1H, J = 2), 7.42 (s, 1H, NC=*H*), 7.27 (m, 2H), 6.9-7.1 (m, 6H), 6.6-6.9 (m, 4H), 4.84 (dd, 1H, *J* = 2, 11, C*H*CH_aH_bPh), 3.57 (s, 6H, (NMe_2)), 3.12 (dd, 1H, *J* = 14, 2, CHC*H*$_a$$H_b$Ph), 2.76 (dd, 1H, *J* 14, 11, CHCH_a*H*$_b$Ph), 1.59 (s, 9H, CMe_3), 1.10 (s, 9H, CMe_3). ^{13}C NMR (100 MHz, C_6D_6): δ 166.41 (C=N), 159.94 (4°), 148.63 (4°), 146.37 (4°), 143.08 (4°), 139.39 (4°), 139.04 (4°), 131.78 (CH), 130.88 (CH), 129.55 (CH), 129.50 (CH), 129.38 (CH), 128.90 (CH), 127.92 (CH), 127.59 (CH), 127.41 (CH), 126.57 (CH), 126.50 (CH), 122.17 (4°), 93.99 (4°), 87.34 (CH), 51.68 (CH_3), 39.26 (CH_2), 36.13 (4°), 34.80 (4°), 31.88 (^{t}Bu), 30.66 (^{t}Bu).

Complex D-14, Ti(D-L6)(NMe_2)Cl

D-H_2**L6** (0.143 g, 0.275 mmol) and $TiCl(NMe_2)_3$ (0.059 g, 0.275 mmol) were each dissolved in 3 mL diethyl ether and cooled to -35°C. The ligand was added dropwise to the metal solution with stirring and diluted to 10 mL with additional diethyl ether. The solution changed color from yellow to red, and then a solid formed which was collected by vacuum filtration (0.140 g, 0.217 mmol, 79% yield). The ^{1}H NMR spectrum of D-**14** matched that of L-**14**.

Typical procedure for chiral shift NMR

Chiral shift studies were performed for all ligands using the following procedure. The L-enantiomer of the ligand (~ 10 mg, ca. 0.05 mmol) was dissolved in $CDCl_3$ (ca. 0.75 mL) and examined by ^{1}H NMR spectroscopy. (*S*)-(+)-2,2,2-Trifluoro-1-(9-anthryl)ethanol (~ 15 mg, 1 equiv.) was added to the solution which was then reexamined by ^{1}H NMR spectroscopy. Additional shift reagent (~15 mg, 1 equiv.) was added and a final spectrum was taken. These procedures were repeated with the D-enantiomer, and then both 2 equiv. samples were combined and a final spectrum was obtained.

Typical procedure for the hydroamination of hepta-4,5-dienylamine

Hydroamination was carried out with 5 mol % catalyst loading. Inside the glove box deuterated benzene (175 μL), $Ti(NMe_2)_4$ (100 μL of a 0.0375 M solution, $3.75 \cdot 10^{-3}$ mmol), ligand (75 μL of a 0.05 M solution, $3.75 \cdot 10^{-3}$ mmol) and hepta-4,5-dienylamine (50 μL of a 1.50 M solution, 0.075 mmol, 20 eq.) were combined in a medium-walled J. Young NMR tube, and a ^{1}H NMR spectrum was taken. The tube was placed in a 110 ± 1 °C oil bath and monitored by ^{1}H NMR until the reaction reached completion or stalled. The *E*/*Z* ratios and percent conversion were determined by comparison with known spectra.[16, 88]

Typical procedure for the hydroamination of 6-methyl-hepta-4,5-dienylamine

Hydroamination was carried out with 5 mol % catalyst loading. Inside the glovebox, deuterated benzene (175 μL), $Ti(NMe_2)_4$ (100 μL of a 0.0375 M solution, 3.75×10^{-3} mmol), ligand (75 μL of a 0.05 M solution, 3.75×10^{-3} mmol), and 6-methyl-hepta-4,5-dienylamine (50 μL of a 1.5 M solution, 0.075 mmol, 20 equiv) were combined in a medium-walled J. Young NMR tube, and an ^{1}H NMR spectrum was taken. The tube was placed in a 135 ± 1 °C oil bath and monitored by ^{1}H NMR until the reaction reached completion or stalled. Percent conversion was determined by ^{1}H NMR spectroscopy.

Typical procedure for derivatization and determination of enantiomeric excess

The J. Young NMR tube of a completed reaction was transferred into a small vial, where benzyl bromide (9 μL, 0.08 mmol) and triethylamine (21 μL, 0.15 mmol) were added. The tube was left to sit for 18 hours and a crystalline solid precipitated out of solution. Isopropanol (100 μL) was added to the solution which was then filtered through glass fibers in a pipette filter. The clear solution was diluted to a total volume of 2 mL with benzene. The crude solution (1 μL) was injected on the GC capillary column (Chiraldex B-DM, 30 m × 0.25 μm, split ratio 400, flow rate 41 cm/sec, 100 °C, 8 min, 1 °C/min to 136 °C, 10 °C/min to 180 °C, hold 20 min). The two enantiomers of *E*-2-propenyl-pyrrolidine were separated with retention times of approximately 34.2 and 35.4 minutes. The two enantiomers of *Z*-2-propenyl-pyrrolidine were separated with retention times of approximately 36.6 and 37.7 minutes. The two enantiomers of 2-(2-methyl-propenyl)-pyrrolidine were separated with retention times of approximately 41.3 and 42.1 min. The absolute stereochemistry of 2-(2-methyl-propenyl)-pyrrolidine is not known with certainty but the preferred isomer is assigned as the *S*-(-)-isomer by comparison to related molecules.[43]

X-ray collection and refinement

Pale yellow, almost colorless crystals of L-H_2**L4**, L-H_2**L6**, L-H_2**L7** and L-H_2**L8** were grown by slow evaporation from 4:1 ether/isopropanol and had dimensions of 0.35 x 0.29 x 0.14 mm^3 (H_2**L4**), 0.20 x 0.20 x 0.20 mm^3 (H_2**L6**), 0.30 x 0.25 x 0.20 mm^3 (H_2**L7**) and 0.17 x 0.12 x 0.08 mm^3 (H_2**L8**) respectively. The crystals were secured to Mitegen micromounts using Paratone oil and their single crystal X-ray diffraction data was collected at 100 K using a Rigaku Oxford Diffraction (ROD) Synergy-S X-ray diffractometer equipped with a HyPix-6000HE hybrid photon counting (HPC) detector and microfocused Cu $K_{\alpha 1}$ radiation (λ = 1.54184 Å). For all samples, data collection strategies to ensure the completeness and redundancy necessary to determine their absolute configurations were determined using CrysAlis^{Pro}.[89] Data processing was done using CrysAlis^{Pro} and included multi-scan absorption corrections on all samples applied using the SCALE3 ABSPACK scaling algorithm.[90] All structures were solved via intrinsic phasing methods using ShelXT[91] and refined using ShelXL[92] in the Olex2 graphical user interface.[93] Space groups were unambiguously verified by PLATON.[94] The final structural refinement included anisotropic temperature factors on all non-hydrogen atoms. Given the quality of the data, all hydrogen atoms were located in the difference map and refined.

Pale yellow crystals of complex **11** were grown from CH_2Cl_2 at -30 °C. Low-temperature diffraction data (ϕ-and ω-scans) were collected on a Bruker AXS D8 VENTURE KAPPA diffractometer coupled to a PHOTON II CPAD detector with Mo K_a radiation (λ = 0.71073 Å) from an IμS micro-source. The structure was solved by direct methods using SHELXS[95] and refined against F^2 on all data by full-matrix least squares with SHELXL-2016[92] using established refinement techniques.[96] All non-hydrogen atoms were refined anisotropically. All hydrogen atoms were included into the model at geometrically calculated positions and refined using a

riding model. The isotropic displacement parameters of all hydrogen atoms were fixed to 1.2 times the *U* value of the atoms they are linked to (1.5 times for methyl groups). All disordered atoms were refined with the help of similarity restraints on the 1,2- and 1,3-distances and displacement parameters as well as enhanced rigid bond restraints for anisotropic displacement parameters.

Thermal ellipsoid plots were generated using CrystalMaker.[97] Crystallographic data for the structures reported in this paper have been deposited with the Cambridge Crystallographic Data Centre (https://www.ccdc.cam.ac.uk) as CCDC 1837506 (L-H_2**L4**), 1837507 (L-H_2**L6**), 1837508 (L-H_2**L7**), 1837509 (L-H_2**L8**), and 1834567 (**11**).

References

1. E. Vitaku, D. T. Smith and J. T. Njardarson, *J. Med. Chem.*, 2014, **57**, 10257-10274.
2. E. Bernoud, C. Lepori, M. Mellah, E. Schulz and J. Hannedouche, *Catal. Sci. Technol.*, 2015, **5**, 2017-2037.
3. J. Hannedouche and E. Schulz, *Chem. Eur. J.*, 2013, **19**, 4972-4985.
4. K. D. Hesp and M. Stradiotto, *ChemCatChem*, 2010, **2**, 1192-1207.
5. T. E. Müller, K. C. Hultzsch, M. Yus, F. Foubelo and M. Tada, *Chem. Rev.*, 2008, **108**, 3795-3892.
6. K. C. Hultzsch, *Adv. Synth. Catal.*, 2005, **347**, 367-391.
7. K. C. Hultzsch, *Org. Biomol. Chem.*, 2005, **3**, 1819-1824.
8. S. Hong and T. J. Marks, *Acc. Chem. Res.*, 2004, **37**, 673-686.
9. F. Pohlki and S. Doye, *Chem. Soc. Rev.*, 2003, **32**, 104-114.
10. E. M. Beccalli, G. Broggini, M. S. Christodoulou and S. Giofrè, in *Advances in Organometallic Chemistry*, ed. P. J. Pérez, Academic Press, 2018, vol. 69, pp. 1-71.
11. H. N. Nguyen, H. Lee, S. Audörsch, A. L. Reznichenko, A. J. Nawara-Hultzsch, B. Schmidt and K. C. Hultzsch, *Organometallics*, 2018, **37**, 4358-4379.
12. J. Hannedouche and E. Schulz, *Organometallics*, 2018, **37**, 4313-4326.
13. K. S. A. Motolko, D. J. H. Emslie and H. A. Jenkins, *Organometallics*, 2017, **36**, 1601-1608.
14. S. Germain, E. Schulz and J. Hannedouche, *ChemCatChem*, 2014, **6**, 2065-2073.
15. A. E. Strom and J. F. Hartwig, *J. Org. Chem.*, 2013, **78**, 8909-8914.
16. V. Arredondo, S. Tian, F. E. McDonald and T. J. Marks, *J. Am. Chem. Soc.*, 1999, **121**, 3633-3639.

17. B. D. Stubbert and T. J. Marks, *J. Am. Chem. Soc.*, 2007, **129**, 6149-6167.
18. P. Chirik and R. Morris, *Acc. Chem. Res.*, 2015, **48**, 2495.
19. A. J. Hunt, T. J. Farmer and J. H. Clark, in *Element Recovery and Sustainability*, The Royal Society of Chemistry, 2013, pp. 1-28.
20. I. Bytschkov and S. Doye, *Eur. J. Org. Chem.*, 2003, 935-946.
21. S. H. Rohjans, J. H. Ross, L. H. Lühning, L. Sklorz, M. Schmidtmann and S. Doye, *Organometallics*, 2018, **37**, 4350-4357.
22. A. L. Reznichenko and K. C. Hultzsch, *Organometallics*, 2010, **29**, 24-27.
23. A. L. Odom, *Dalton Trans.*, 2005, 225-233.
24. S. Majumder and A. L. Odom, *Organometallics*, 2008, **27**, 1174-1177.
25. D. L. Swartz Ii, R. J. Staples and A. L. Odom, *Dalton Transactions*, 2011, **40**, 7762-7768.
26. K. E. Aldrich and A. L. Odom, *Organometallics*, 2018, **37**, 4341-4349.
27. T. S. Brunner, L. Hartenstein and P. W. Roesky, *J. Organometal. Chem.*, 2013, **730**, 32-36.
28. L. Hussein, N. Purkait, M. Biyikal, E. Tausch, P. W. Roesky and S. Blechert, *Chem. Commun.*, 2014, **50**, 3862-3864.
29. K. Manna, W. C. Everett, G. Schoendorff, A. Ellern, T. L. Windus and A. D. Sadow, *J. Am. Chem. Soc.*, 2013, **135**, 7235-7250.
30. K. Manna, N. Eedugurala and A. D. Sadow, *J. Am. Chem. Soc.*, 2015, **137**, 425-435.
31. S. A. Ryken and L. L. Schafer, *Acc. Chem. Res.*, 2015, **48**, 2576-2586.
32. C. Braun, S. Bräse and L. L. Schafer, *Eur. J. Org. Chem.*, 2017, **2017**, 1760-1764.
33. H. Hao, K. A. Thompson, Z. M. Hudson and L. L. Schafer, *Chemistry – A European Journal*, 2017, **24**, 5562-5568.
34. E. K. J. Lui, J. W. Brandt and L. L. Schafer, *J. Am. Chem. Soc.*, 2018, **140**, 4973-4976.
35. X. Zhou, B. Wei, X.-L. Sun, Y. Tang and Z. Xie, *Chem. Commun.*, 2015, **51**, 5751-5753.
36. X. Wang, Z. Chen, X.-L. Sun, Y. Tang and Z. Xie, *Org. Lett.*, 2011, **13**, 4758-4761.
37. C. Michon, M.-A. Abadie, F. Medina and F. Agbossou-Niedercorn, *J. Organometal. Chem.*, 2017, **847**, 13-27.
38. Z. W. Davis-Gilbert and I. A. Tonks, *Dalton Transactions*, 2017, **46**, 11522-11528.
39. A. J. Pearce, X. Y. See and I. A. Tonks, *Chem. Commun.*, 2018, **54**, 6891-6894.
40. H.-C. Chiu and I. A. Tonks, *Angewandte Chemie International Edition*, 2018, **57**, 6090-6094.
41. J. M. Hoover, J. R. Petersen, J. H. Pikul and A. R. Johnson, *Organometallics*, 2004, **23**, 4614-4620.
42. A. J. Hickman, L. D. Hughs, C. M. Jones, H. Li, J. E. Redford, S. J. Sobelman, J. A. Kouzelos and A. R. Johnson, *Tetrahedron: Asymmetry*, 2009, **20**, 1279-1285.
43. M. C. Hansen, C. A. Heusser, T. C. Narayan, K. E. Fong, N. Hara, A. W. Kohn, A. R. Venning, A. L. Rheingold and A. R. Johnson, *Organometallics*, 2011, **30**, 4616-4623.
44. K. E. Near, B. M. Chapin, D. C. McAnnally-Linz and A. R. Johnson, *J. Organometal. Chem.*, 2011, **696**, 81-86.
45. R. L. LaLonde, B. D. Sherry, E. J. Kang and F. D. Toste, *J. Am. Chem. Soc.*, 2007, **129**, 2452-2453.
46. T. E. Müller, K. C. Hultzsch, M. Yus, F. Foubelo and M. Tada, *Chem. Rev.*, 2008, **108**, 3795-3892.
47. B. Alcaide and P. Almendros, *Adv. Synth. Catal.*, 2011, **353**, 2561-2576.

48. J. C. McWilliams, 2015.
49. L. Liu, H.-C. Wu and J.-Q. Yu, *Chem. - Eur. J.*, 2011, **17**, 10828-10831, S10828/10821-S10828/10821.
50. P. T. Anastas and J. C. Warner, *Green chemistry: theory and practice*, Oxford University Press, New York, 1998.
51. H.-U. Blaser, *Chem. Rev.*, 1992, **92**, 935-952.
52. C. Ho, S. Herron, K. Kantardjieff and A. Johnson, *Journal*, 2002, **341**, 71-76.
53. J. R. Petersen, J. M. Hoover, W. S. Kassel, A. L. Rheingold and A. R. Johnson, *Inorg. Chim. Acta*, 2005, **358**, 687-694.
54. M. Green, *J. Organomet. Chem.*, 1995, **500**, 127-148.
55. P. G. Cozzi, *Chem. Soc. Rev.*, 2004, **33**, 410-421.
56. C. J. Whiteoak, G. Salassa and A. W. Kleij, *Chem. Soc. Rev.*, 2012, **41**, 622-631.
57. S.-H. Hsieh, Y.-P. Kuo and H.-M. Gau, *Dalton Transactions*, 2007, 97-106.
58. N. Ananthi and S. Velmathi, *Advanced Science Letters*, 2012, **17**, 233-237.
59. G.-R. Qiang, T.-H. Shen, X.-C. Zhou, X.-X. An and Q.-B. Song, *Chirality*, 2014, **26**, 780-783.
60. M. Hayashi, Y. Miyamoto, T. Inoue and N. Oguni, *J. Org. Chem.*, 1993, **58**, 1515-1522.
61. Q. Tian, C. Jiang, Y. Li, C. Jiang and T. You, *J. Mol. Catal. A: Chem.*, 2004, **219**, 315-317.
62. Y.-F. Kang, L. Liu, R. Wang, W.-J. Yan and Y.-F. Zhou, *Tetrahedron: Asymmetry*, 2004, **15**, 3155-3159.
63. L. Liu, Y.-f. Kang, R. Wang, Y.-f. Zhou, C. Chen, M. Ni and M.-z. Gong, *Tetrahedron: Asymmetry*, 2004, **15**, 3757-3761.
64. F. Liu, X. Bugaut, M. Schedler, R. Fröhlich and F. Glorius, *Angewandte Chemie International Edition*, 2011, **50**, 12626-12630.
65. W. H. Pirkle, D. L. Sikkenga and M. S. Pavlin, *J. Org. Chem.*, 1977, **42**, 384-387.
66. E. W. Reinheimer, A. W. Kohn, R. H. Groeneman, H. R. Krueger, K. Kantardjieff and A. R. Johnson, *Mol. Cryst. Liq. Cryst.*, 2016, **629**, 70-77.
67. E. W. Reinheimer, A. J. Hickman, J. E. Moretti, X. Ouyang, K. A. Kantardjieff and A. R. Johnson, *J. Chem. Crystallogr.*, 2012, **42**, 911-915.
68. S. M. Lee, K. M. Lo, S. L. Tan and E. R. T. Tiekink, *Acta Crystallographica Section E*, 2016, **72**, 1223-1227.
69. M. Salehi, F. Ghasemi, M. Kubicki, A. Asadi, M. Behzad, M. H. Ghasemi and A. Gholizadeh, *Inorg. Chim. Acta*, 2016, **453**, 238-246.
70. M. J. Frisch, G. W. Trucks, H. B. Schlegel, G. E. Scuseria, M. A. Robb, J. R. Cheeseman, G. Scalmani, V. Barone, B. Mennucci, G. A. Petersson, H. Nakatsuji, M. Caricato, X. Li, H. P. Hratchian, A. F. Izmaylov, J. Bloino, G. Zheng, J. L. Sonnenberg, M. Hada, M. Ehara, K. Toyota, R. Fukuda, J. Hasegawa, M. Ishida, T. Nakajima, Y. Honda, O. Kitao, H. Nakai, T. Vreven, J. J. A. Montgomery, J. E. Peralta, F. Ogliaro, M. Bearpark, J. J. Heyd, E. Brothers, K. N. Kudin, V. N. Staroverov, T. Keith, R. Kobayashi, J. Normand, K. Raghavachari, A. Rendell, J. C. Burant, S. S. Iyengar, J. Tomasi, M. Cossi, N. Rega, J. M. Millam, M. Klene, J. E. Knox, J. B. Cross, V. Bakken, C. Adamo, J. Jaramillo, R. Gomperts, R. E. Stratmann, O. Yazyev, A. J. Austin, R. Cammi, C. Pomelli, J. W. Ochterski, R. L. Martin, K. Morokuma, V. G. Zakrzewski, G. A. Voth, P. Salvador, J. J. Dannenberg, S. Dapprich, A. D. Daniels, O. Farkas, J. B. Foresman, J. V. Ortiz, J.

Cioslowski and D. J. Fox, *Gaussian 09 (Revision D.01)*, Gaussian, Inc., Wallingford, CT, 2013.
71. R. Fleischer, H. Wunderlich and M. Braun, *Eur. J. Org. Chem.*, 1998, **1998**, 1063-1070.
72. R. D. Chakravarthy, K. Suresh, V. Ramkumar and D. K. Chand, *Inorg. Chim. Acta*, 2011, **376**, 57-63.
73. A. W. Addison, T. N. Rao, J. Reedijk, J. van Rijn and G. C. Verschoor, *Journal of the Chemical Society, Dalton Transactions*, 1984, 1349-1356.
74. J. W. Yao, R. C. B. Copley, J. A. K. Howard, F. H. Allen and W. D. S. Motherwell, *Acta Cryst.*, 2001, **B57**, 251-260.
75. M. Jaworska, P. B. Hrynczyszyn, M. Wełniak, A. Wojtczak, K. Nowicka, G. Krasiński, H. Kassassir, W. Ciesielski and M. J. Potrzebowski, *The Journal of Physical Chemistry A*, 2010, **114**, 12522-12530.
76. A. Akıncı, B. Celepci Duygu, L. Karadeniz, N. Korkmaz, M. Aygün and T. Astley Stephen, *Applied Organometallic Chemistry*, 2017, **31**, e3831.
77. K. Yanagi and M. Minobe, *Acta Crystallographica Section C*, 1987, **43**, 1045-1048.
78. K. Yanagi and M. Minobe, *Acta Crystallographica Section C*, 1987, **43**, 2060-2063.
79. F. Guo, D. Chang, G. Lai, T. Zhu, S. Xiong, S. Wang and Z. Wang, *Chemistry – A European Journal*, 2011, **17**, 11127-11130.
80. K. Gräbe, F. Pohlki and S. Doye, *Eur. J. Org. Chem.*, 2008, **2008**, 4815-4823.
81. V. Arredondo, F. E. McDonald and T. J. Marks, *Organometallics*, 1999, **18**, 1949-1960.
82. R. C. Larock, H. Yang, S. M. Weinreb and R. J. Herr, *J Org Chem*, 1994, **59**, 4172-4178.
83. C. Welter, A. Dahnz, B. Brunner, S. Streiff, P. Dubon and G. Helmchen, *Org Lett*, 2005, **7**, 1239-1242.
84. J. A. Seijas, M. P. Vazqueztato, L. Castedo, R. J. Estevez, M. G. Onega and M. Ruiz, *Tetrahedron*, 1992, **48**, 1637-1642.
85. H. Nagashima, M. Gondo, S. Masuda, H. Kondo, Y. Yamaguchi and K. Matsubara, *Chem. Commun.*, 2003, 442-443.
86. D. D. Perrin and L. F. Armarego, *Purification of Laboratory Chemicals*, Pergamon Press, New York, 1988.
87. M. Çolak and N. Demirel, *Tetrahedron: Asymmetry*, 2008, **19**, 635-639.
88. V. Arredondo, F. E. McDonald and T. J. Marks, *J. Am. Chem. Soc.*, 1998, **120**, 4871-4872.
89. CrysAlisPro, Rigaku Oxford Diffraction, version 171.39.33b, 2017.
90. SCALE3 ABSPACK — A Rigaku Oxford Diffraction program for Absorptin Corrections, Rigaku Oxford Diffraction, 2017.
91. G. M. Sheldrick, *Acta Cryst.*, 2015, **A64**, 3-8.
92. G. M. Sheldrick, *Acta Cryst.*, 2015, **C71**, 3-8.
93. O. V. Dolomanov, L. J. Bourhis, R. J. Gildea, J. A. K. Howard and H. Puschmann, *Journal of Applied Crystallography*, 2009, **42**, 339-341.
94. A. Spek, *Acta Crystallographica Section D*, 2009, **65**, 148-155.
95. G. Sheldrick, *Acta Crystallographica Section A*, 1990, **46**, 467-473.
96. P. Müller, *Crystallography Reviews*, 2009, **15**, 57-83.
97. Crystalmaker, CrystalMaker Software Ltd, Oxford, England (www.crystalmaker.com), 10.2.2, 2018.